Published OnlineFirst November 7, 2014; DOI: 10.1158/0008-5472.CAN-13-3686

Cancer Research

B-Raf Inhibitors Induce Epithelial Differentiation in *BRAF*-Mutant Colorectal Cancer Cells

Ricarda Herr[1,2], Martin Köhler[1,2,3], Hana Andrlová[4], Florian Weinberg[1,2], Yvonne Möller[5], Sebastian Halbach[1,2,3], Lisa Lutz[6], Justin Mastroianni[2,4], Martin Klose[7], Nicola Bittermann[6], Silke Kowar[7], Robert Zeiser[4,8], Monilola A. Olayioye[5], Silke Lassmann[6,8,9,10], Hauke Busch[7,9,10], Melanie Boerries[7,9,10], and Tilman Brummer[1,8]

Abstract

BRAF mutations are associated with aggressive, less-differentiated and therapy-resistant colorectal carcinoma. However, the underlying mechanisms for these correlations remain unknown. To understand how oncogenic B-Raf contributes to carcinogenesis, in particular to aspects other than cellular proliferation and survival, we generated three isogenic human colorectal carcinoma cell line models in which we can dynamically modulate the expression of the B-Raf^{V600E} oncoprotein. Doxycyclin-inducible knockdown of endogenous B-Raf^{V600E} decreases cellular motility and invasion in conventional and three-dimensional (3D) culture, whereas it promotes cell–cell contacts and induces various hallmarks of differentiated epithelia. Importantly, all these effects are recapitulated by B-Raf (PLX4720, vemurafenib, and dabrafenib) or MEK inhibitors (trametinib). Surprisingly, loss of B-Raf^{V600E} in HT29 xenografts does not only stall tumor growth, but also induces glandular structures with marked expression of *CDX2*, a tumor-suppressor and master transcription factor of intestinal differentiation. By performing the first transcriptome profiles of PLX4720-treated 3D cultures of HT29 and Colo-205 cells, we identify several upregulated genes linked to epithelial differentiation and effector functions, such as claudin-1, a Cdx-2 target gene encoding a critical tight junction component. Thereby, we provide a mechanism for the clinically observed correlation between mutant *BRAF* and the loss of Cdx-2 and claudin-1. PLX4720 also suppressed several metastasis-associated transcripts that have not been implicated as targets, effectors or potential biomarkers of oncogenic B-Raf signaling so far. Together, we identify a novel facet of clinically applied B-Raf or MEK inhibitors by showing that they promote cellular adhesion and differentiation of colorectal carcinoma cells. *Cancer Res; 75(1); 1–14. ©2014 AACR.*

Introduction

Colorectal carcinomas are characterized by a series of (epi) genetic alterations, including aberrant Wnt pathway activity and gain-of-function mutations in the *KRAS* or *BRAF* proto-oncogenes. Compared with advances in deciphering the events initiating colorectal carcinoma, little is known about the mechanisms underlying metastasis (1, 2). However, there is a pressing need to better understand and target metastatic colorectal carcinoma.

BRAF encodes a Ser/Thr kinase of the Ras/MEK/ERK pathway and is mutated in various tumor entities. The most common mutation, V600E, renders the kinase constitutively active and occurs in 11% of colorectal carcinoma (3). *BRAF* mutations are implicated as early "signature events" in the so-called serrated pathway describing the progression from serrated adenoma to colorectal carcinomas (2, 4). Importantly, *BRAF*-mutant colorectal carcinomas can be subdivided in two subgroups that differ in terms of microsatellite stability (MSS) and clinical outcome (5). The majority of *BRAF*-mutant colorectal carcinomas belong to the microsatellite instable (MSI) class, which poses the lowest risk for relapse of all colorectal carcinoma subtypes (6, 7). However, *BRAF*-mutant colorectal carcinomas with MSS represents a very aggressive entity and forecast a poor prognosis (8–10). Interestingly, *BRAF*-mutant colorectal carcinomas present with a distinct pattern of metastatic spread, in particular peritoneal carcinomatosis, and a shorter overall survival even after metastasectomy (11, 12).

The discovery of B-Raf^{V600E} has been translated into clinically applied kinase inhibitors, such as vemurafenib or dabrafenib. As single agents, they yield unprecedented responses in *BRAF*-mutant melanoma (13, 14). However, such an efficacy was not

[1]Signal Transduction in Tumour Development and Drug Resistance Group, Institute of Molecular Medicine and Cell Research (IMMZ), Albert-Ludwigs-University (ALU), Freiburg, Germany. [2]Faculty of Biology, ALU, Freiburg, Germany. [3]Spemann Graduate School of Biology and Medicine (SGBM), ALU, Freiburg, Germany. [4]Department of Hematology and Oncology, University Medical Center, ALU, Freiburg, Germany. [5]Institute of Cell Biology and Immunology, University of Stuttgart, Stuttgart, Germany. [6]Department of Pathology, University Medical Center, ALU, Freiburg, Germany. [7]Systems Biology of the Cellular Microenvironment Group, IMMZ, ALU, Freiburg, Germany. [8]Centre for Biological Signalling Studies *BIOSS*, ALU Freiburg. [9]German Cancer Consortium (DKTK), Freiburg, Germany. [10]German Cancer Research Center (DKFZ), Heidelberg, Germany.

Note: Supplementary data for this article are available at Cancer Research Online (http://cancerres.aacrjournals.org/).

Corresponding Author: Tilman Brummer, Institute of Molecular Medicine and Cell Research (IMMZ), Faculty of Medicine, Albert-Ludwigs-University Freiburg, Stefan-Meier-Strasse 17, Freiburg 79104, Germany. Phone: 49-761-203-9610; Fax: 49-761-203-9602; E-mail: tilman.brummer@zbsa.de

doi: 10.1158/0008-5472.CAN-13-3686

Published OnlineFirst November 7, 2014; DOI: 10.1158/0008-5472.CAN-13-3686

observed in the small groups of 21 patients with colorectal carcinoma treated with these compounds. Nevertheless, these inhibitors still elicited partial responses and stabilized disease in some patients (14, 15). Depending on their mutational landscape, *BRAF*-mutant colorectal carcinoma cell lines display differential sensitivity toward B-Raf or MEK inhibitors in tissue culture and xenograft models (4, 13, 16–18). Thus, these compounds still hold clinical promise, in particular if their combination with other substances is considered and once the complex pathology and genetic heterogeneity of colorectal carcinoma are better understood. Indeed, combination strategies show efficacy in preclinical colorectal carcinoma models as they target more than one critical node for proliferation and survival. These approaches prevent compensatory feedback loops and crosstalk, which currently limit the use of B-Raf inhibitors as single agents (4, 19–21). These preclinical drug combinations initiated several clinical trials that are currently ongoing (www.clinicaltrials.gov) and a first case report further demonstrates the utility of such combinations (22). However, to interpret the effect of such combinatorial approaches, it is necessary to obtain a more comprehensive understanding of their effects as monosubstances. Herein, we characterize three isogenic colorectal carcinoma cell line models in which B-Raf^{V600E} can be dynamically modulated. We demonstrate that B-Raf^{V600E} controls promigratory and proinvasive effectors and suppresses hallmarks of intestinal differentiation. Importantly, we report that clinically relevant B-Raf and MEK inhibitors mimic the effects of B-Raf^{V600E} depletion, suggesting that they promote a more differentiated and adhesive state, which in turn might improve prognosis and drug response.

Materials and Methods

Tissue culture

Short tandem repeat–authenticated Colo-205 cells were purchased from CLS Cell Lines Service GmbH (Heidelberg, Germany) and cultured in RPMI-1640 with 10% FCS. Total passage time was under 6 months. Caco-2 and HT29 sublines and associated recombinant DNAs were described previously (23). All other lines were kindly provided by Stephan Feller (Martin-Luther-University Halle-Wittenberg, Germany) and cultivated like HT29 cells. Except for Colo-205, the identity of all lines was confirmed by SNP analysis (Multiplexion) in June 2014. Three-dimensional (3D) cultures were set-up in their culture medium as described previously (24). Details on cellular assays (clonogenic, wound healing, migration, and invasion as well as cell-cycle analyses) are described in Supplementary Data. Organotypic collagen I assays were set-up as described previously (25).

Inhibitors and inducers

The following inhibitors were dissolved in DMSO: PLX4720 (Santa Cruz Biotechnology), dabrafenib, trametinib, vemurafenib (PLX4032), and gefitinib were purchased from Selleck Chemicals. Doxycycline was used at 2 μg/mL (24).

Immunofluorescence

Immunofluorescence microscopy was conducted as described previously (24) using the antibody manufacturers' instructions. Topro-3 iodide was used as counterstain and bound primary antibodies were detected using the secondary antibodies Alexa Fluor 488 goat-anti-mouse IgG and Alexa Fluor 488 goat-anti-rabbit IgG (Invitrogen).

Western blotting

Western blotting was performed as described previously (23, 24). Detailed information on antibodies is provided in Supplementary Data. Blotted proteins were visualized with a Fusion Solo chemiluminescence reader and quantified using FusionCapt software (Vilber Lourmat).

Rac1 pulldown

Pulldown assays were conducted as described previously (26). PLX4720 or DMSO was added daily.

Xenografts

All procedures were carried out in accordance with local animal ethics committees (G-12/34 and G-13/116). Subcutaneous xenografts were generated by injecting 1×10^6 HT29 cells (in 100 μL PBS) into severely immunocompromised *Rag2*$^{-/-}$;γc$^{-/-}$ mice. Once tumors became measurable at d7, mice were randomly distributed to treatment groups and received doxycycline (2 mg/mL) via sucrose-supplemented (35 g/L) drinking water or not. Inhibitors were applied by oral gavage as indicated. Tumors were measured with calipers and subjected to histologic processing. Formalin-fixed and paraffin-embedded xenograft tumors were cut (3 μm), deparaffinized, subjected to standard operating procedures-driven antigen retrieval and antibody staining (primary antibodies for CK20, Cdx-2, PAS, Ki67, and secondary reagents according to routine diagnostic procedures) in a DAKO autostainer.

RNA isolation and time-resolved microarray analysis

RNA was extracted using the Universal RNA Purification Kit (GeneMatrix) from Roboklon. RNA quality and integrity was verified using the Agilent 2100 Bioanalyzer system (Agilent Technologies). Transcript profiling is described in detail in Supplementary Data. Gene-expression data are available at GEO using the following link http://www.ncbi.nlm.nih.gov/geo/query/acc.cgi?token=edcfcmuszbudrst&acc=GSE50791.

Statistical analysis

Quantitative data are presented as mean ± SE. Multiple group and pair-wise comparisons were performed by ANOVA or the Student *t* test (two-tailed), respectively. A *P* value of ≤ 0.05 was considered statistically significant (***, $P < 0.001$; **, $P < 0.01$; and *, $P < 0.05$). Unless noted otherwise, bar diagrams report the mean of three independent experiments. Statistics of transcriptome data are described in Supplementary Data.

Results

Establishment of conditional B-Raf^{V600E} knockdown systems

To evaluate endogenous B-Raf^{V600E} for its contribution to the phenotype of human colorectal carcinoma cell lines within an isogenic background, we generated conditional cell line models. For this approach, we chose two model cell lines, HT29 and Colo-205. Both lines display MSS (Supplementary Table S1), and are therefore likely derived from tumors belonging to the aforementioned high relapse risk subgroup. HT29 was generated from a primary colonic adenocarcinoma (Dukes stage B) and represents a

Published OnlineFirst November 7, 2014; DOI: 10.1158/0008-5472.CAN-13-3686

"moderately differentiated" cell line characterized by growth in epithelial sheets. HT29 cells express E-cadherin but lack tight junctions (TJ; ref. 27). In contrast, the poorly differentiated Colo-205 cells represent metastatic cells derived from ascites of a patient with Duke's stage D colon carcinoma. Both lines were transduced with a nonsilencing control or two pTRIPZ constructs (3_11 and 1_14) allowing the doxycycline-regulated knockdown of B-Raf^{V600E} but not of B-Raf^{wt} (23). All experiments in the main figures were performed with the construct 3_11, key experiments are also shown with 1_14 (Supplementary Data).

B-Raf^{V600E} enhances migration and suppresses the epithelial function of colorectal carcinoma lines derived from primary tumors

First, we evaluated the characteristics of HT29 cells in conventional two-dimensional (2D) culture following B-Raf^{V600E} knockdown. Commensurate with our finding that B-Raf^{V600E} knockdown strongly reduces MEK/ERK phosphorylation in HT29 cells (23), colony growth was impaired, and cells accumulated in the G_1-phase (Fig. 1A and B). However, neither gross morphologic changes nor a significant increase in cell death were

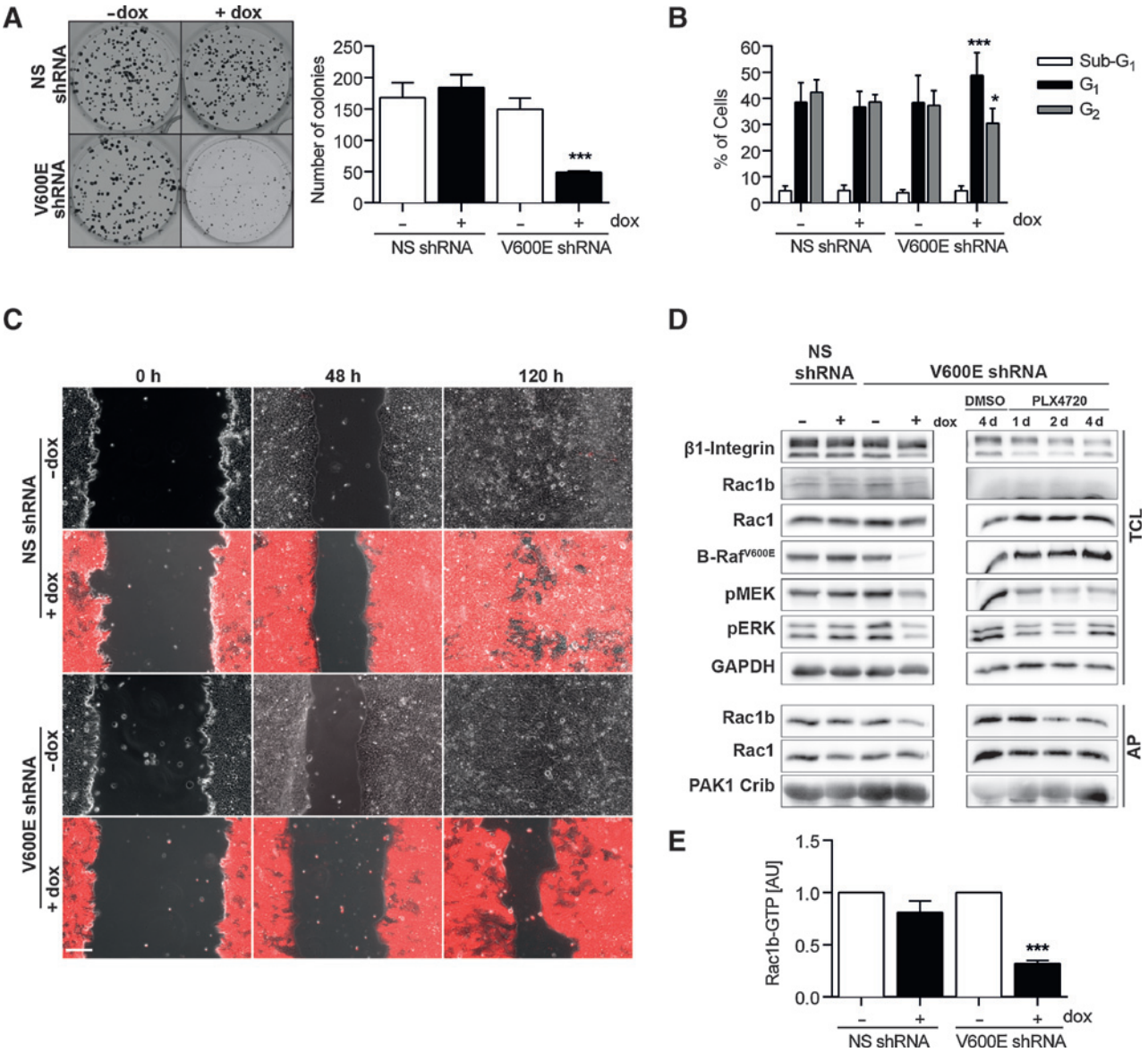

Figure 1.
B-Raf^{V600E} knockdown reduces proliferation and migration in HT29 cells. A, left, colony-forming assay with cells stably expressing inducible nonsilencing (NS) shRNA or B-Raf^{V600E} shRNAs. Cells were treated with ± doxycyclin (dox) for 8 days and stained with Giemsa. Right, statistical analysis, ***, $P < 0.001$. B, cell-cycle analysis of HT29 pools pretreated ±dox for 4 days; statistical analysis, ***, $P < 0.001$; *, $P < 0.05$. C, wound-healing assay. Representative merged fluorescence and phase-contrast images of three independent experiments show wounded cell monolayers at the indicated hours ±dox; scale bar, 200 μm. D, pull-down assay for GTP-loaded Rac1-GTPases. Knockdown was induced for 4 days or cells were treated with 1 μmol/L PLX4720 or DMSO for up to 4 days, respectively. Top, total cellular lysates (TCL); bottom, the corresponding affinity purification (AP). E, statistical analysis of Rac1b-GTP levels, ***, $P < 0.001$.

Published OnlineFirst November 7, 2014; DOI: 10.1158/0008-5472.CAN-13-3686

observed upon B-Raf^{V600E} knockdown (Supplementary Fig. S1A and S1B). Nevertheless, B-Raf^{V600E} knockdown specifically impaired migration (Fig. 1C). Conversely, ectopically expressed B-Raf^{V600E} induced an elongated morphology, faster spreading, and enhanced cell migration of Caco-2 cells, another line derived from a MSS adenocarcinoma (Supplementary Fig. S1C–S1F). This prompted us to analyze the expression of β-integrin subunits in both cell lines. Indeed, B-Raf induced β1- and β4-integrin in Caco-2 cells (Supplementary Fig. S1G), whereas B-Raf^{V600E} knockdown and the vemurafenib tool compound PLX4720 slightly reduced β1-integrin levels in HT29 cells (Fig. 1D). Given the link between Rac-GTPases and integrins, we next evaluated the influence of oncogenic B-Raf on the activation of Rac-1 and its splice variant Rac1b, which is linked to aggressive colorectal carcinoma behavior (28). Knockdown of B-Raf^{V600E} did not affect Rac1-GTP levels, but was accompanied by a significant reduction of Rac1b-GTP (Fig. 1D and E and Supplementary Fig. S2A).

The impact of cancer-associated mutations is increasingly studied using 3D tissue culture (24, 29). For example, Caco-2 cells are widely used to study epithelial effector functions and form cysts in 3D culture. Their single lumen can be enlarged by cholera toxin (CTX)–mediated increase in cyst fluid volume, an event that requires intact TJ and therefore reflects their functionality (29). To study the relevance of B-Raf^{V600E} signaling for the behavior of HT29 cells in 3D culture, single cells were seeded into Matrigel and assayed similarly to Caco-2 cysts (Fig. 2A; refs. 23, 29). In sharp contrast with Caco-2 cysts, CTX did not induce large lumina in HT29 spheroids in untreated or doxycycline-treated nonsilencing cells. Strikingly, spheroids with B-Raf^{V600E} knockdown reacted toward CTX treatment with the formation of large lumina (Fig. 2B and Supplementary Fig. S2B). Importantly, this phenotype was reproduced by administration of PLX4720, vemurafenib, dabrafenib, and the MEK inhibitor trametinib (Fig. 2C and Supplementary Fig. S2C). In contrast, the EGFR inhibitor gefitinib showed no effect on 3D morphology and lumen formation and did not further enhance the effects in combination with PLX4720. This indicates that inhibition of the B-Raf/MEK axis is necessary and sufficient for lumen formation and is not influenced by the crosstalk between the EGFR and oncogenic B-Raf (19, 20). Thus, depletion or pharmacologic inhibition of B-Raf^{V600E} enables HT29 spheroids to respond to CTX with the formation of large lumina.

Next, we analyzed the effect of B-Raf^{V600E} knockdown or inhibition on signaling in 3D cultures. As confirmed by Fig. 2D, induction of the V600E-specific shRNA strongly reduced B-Raf^{V600E} expression as well as MEK/ERK phosphorylation, both of which were not affected by CTX (Supplementary Fig. S2D). Likewise, PLX4720 markedly reduced MEK phosphorylation demonstrating potent B-Raf inhibition. However, ERK phosphorylation was mildly affected in PLX4720-treated cells compared with those with B-Raf^{V600E} knockdown. Nevertheless, the comparable reduction of the well-established ERK target gene product DUSP6, which integrates ERK activity over longer periods of time (30), confirms that PLX4720 had a long-lasting effect on ERK activity. In fact, loss of DUSP6 could increase the half-life of pERK in cells with B-Raf^{V600E} knockdown or inhibition explaining the differential effects on pMEK and pERK levels. In any case, the strong reduction in pMEK levels argues against the paradoxical ERK activation described for B-Raf inhibitors (23). We exclude waning PLX4720 concentrations in the long-term cultures as an explanation for pERK persistence since readdition of PLX4720 1 hour before lysis did not further reduce pERK levels (Supplementary Fig. S2E).

In agreement with the unchanged E-cadherin staining, no considerable alteration in E-cadherin expression was observed. However, β1-integrin was again reduced in B-Raf^{V600E}–depleted or –inhibited spheroids (Fig. 2D), which reflects our results of Caco-2tet and HT29 2D cultures. Collectively, we show that B-Raf^{V600E} increases the motility of HT29 and Caco-2 cells in 2D culture, controls promigratory molecules like Rac1b and β1-integrin, and enables HT29 spheroids to respond to CTX with lumina formation.

Loss of B-Raf^{V600E} signaling restores cell–cell adhesion of metastatic Colo-205 cells and reduces their invasive potential

Next, we analyzed the effects of B-Raf^{V600E} knockdown or inhibition in Colo-205 cells. In 2D culture, loss of B-Raf^{V600E} led to a 3-fold increase in cell death (Supplementary Fig. S2F and S2G). Within the time frame of this experiment, the cells maintained their typical "lymphocytic" morphology (Supplementary Fig. S3A).

Subsequently, we analyzed the importance of B-Raf^{V600E} for the 3D phenotype of Colo-205 cells. Without doxycycline, Colo-205 cells containing either the nonsilencing or the V600E-specific shRNA grew as loose clusters showing a weak and diffuse staining of E-cadherin (Fig. 3A) and β-catenin (Supplementary Fig. S3B). Importantly, B-Raf^{V600E} knockdown caused the formation of compact spheroids with defined membranous E-cadherin or β-catenin localization. Analysis of 3D lysates revealed that E-cadherin was also increased on the protein level (Fig. 3B). This suggests that B-Raf^{V600E} confers the dispersive phenotype of Colo-205 cells in 3D culture and counteracts the function of adherens junctions (AJ). Indeed, PLX4720 and the clinically relevant inhibitors vemurafenib, dabrafenib, or trametinib induced a highly comparable "compaction" phenotype (Fig. 3C and D). However, gefitinib did not provoke such an effect. Thus, the "compaction" phenotype is specifically caused by loss of B-Raf^{V600E} expression, activity or downstream signaling.

As p120ctn stabilizes AJ by blocking E-cadherin endocytosis (31), we addressed the subcellular localization of this catenin relative in Colo-205 cells. In full agreement with our hypothesis that B-Raf^{V600E} impairs AJs, membranous localization of p120ctn was markedly increased upon oncoprotein knockdown or inhibition (Fig. 4A). This increase in membrane-associated p120ctn was correlated with its enhanced phosphorylation at Y228, a marker for its incorporation into AJs (31), in lysates from doxycycline- or PLX4720-treated Colo-205 spheroids (Fig. 4B).

Next, we monitored additional signaling events in the lysates from 3D cultures with B-Raf^{V600E} knockdown (Fig. 3B) or inhibition (Supplementary Fig. S3C). As seen for HT29 cells, doxycycline treatment markedly reduced B-Raf^{V600E} expression and MEK/ERK phosphorylation. We also noted that Rac1b-GTP, which is implicated as a negative regulator of E-cadherin–mediated cell–cell adhesion and as a promoter of cell motility (28), was markedly reduced by B-Raf^{V600E} knockdown in 2D culture (Fig. 4C and D and Supplementary Fig. S3D). This prompted us to analyze the effect of B-Raf^{V600E} on migration and invasion. This showed that vemurafenib significantly reduced both Transwell migration and invasion (Fig. 4E and F). In a 3D organotypic collagen I assay (25), Colo-205 cells with B-Raf^{V600E} knockdown failed to invade the matrix, whereas their untreated isogenic

Published OnlineFirst November 7, 2014; DOI: 10.1158/0008-5472.CAN-13-3686

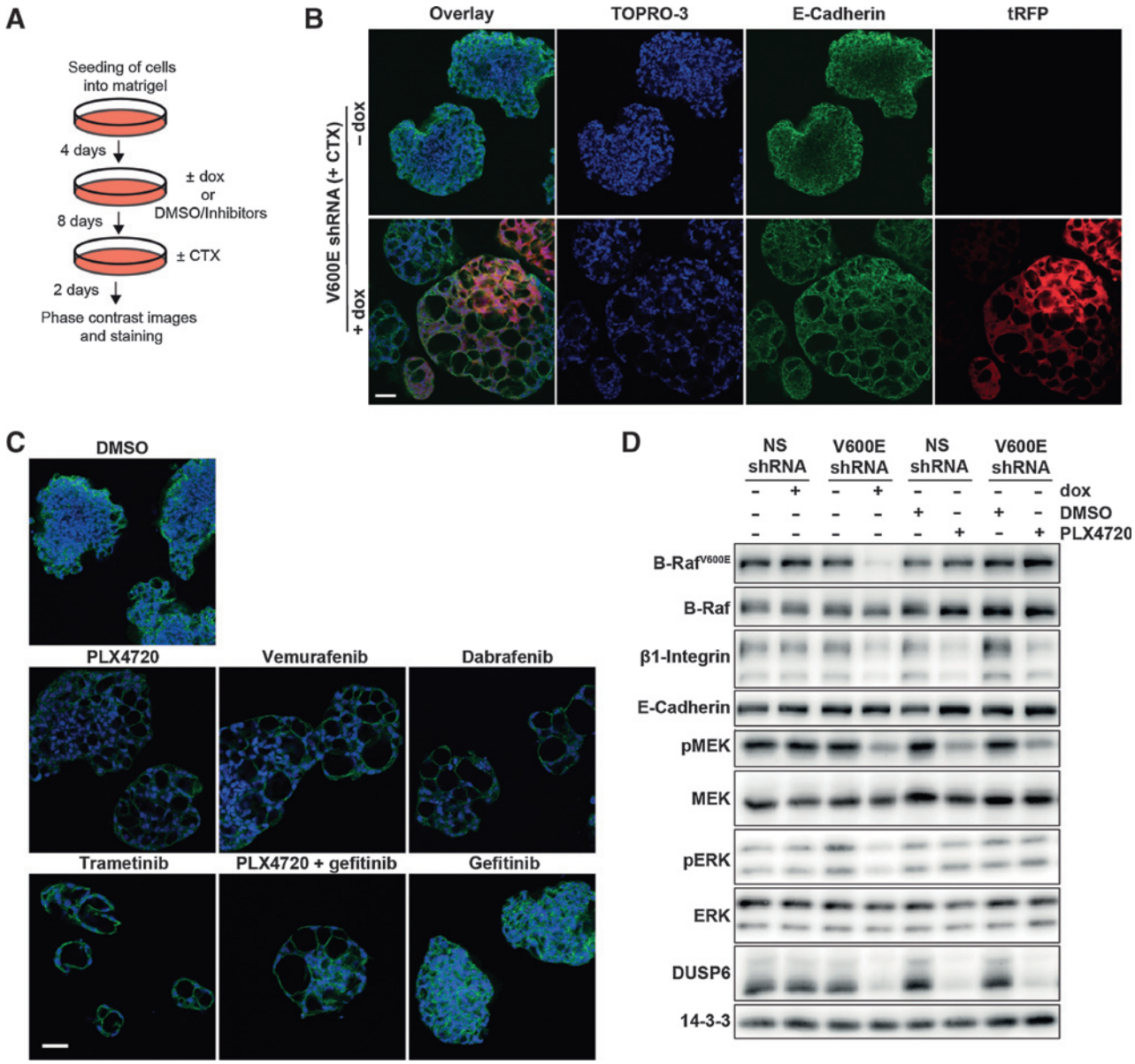

Figure 2.
Inhibition of endogenous B-Raf^{V600E} improves CTX-induced lumen formation in 3D cultures of HT29 cells. A, set-up applied to B–D. B, confocal images of HT29 cells containing the V600E-specific shRNA construct (±doxycyclin, dox) were stained with E-cadherin antibodies and TOPRO-3. Turbo RFP (tRFP) expression indicates shRNA expression. Scale bar, 50 μm. C, merged images showing Topro-3, E-cadherin, and tRFP signals of cells containing the V600E-specific shRNA (−dox) following treatment with PLX4720 (3 μmol/L), vemurafenib (3 μmol/L), dabrafenib (1 μmol/L), trametinib (50 nmol/L), gefitinib (1 μmol/L), or DMSO; scale bar, 50 μm. D, Western blot analysis of 3D cultures exposed to doxycyclin or treated with 3 μmol/L PLX4720 and their corresponding controls (−dox/DMSO).

counterparts or cells expressing the nonsilencing shRNA were detectable in deep layers of the plug (Fig. 4G).

B-Raf^{V600E} inhibition induces a transcript signature correlated with better clinical prognosis

Next, we performed a time-resolved microarray analysis to investigate the transcriptome changes induced by B-Raf inhibition (see Supplementary Fig. S4A and S4B and Supplementary Table S2 for principal component/correlation analysis and a list of all regulated genes, respectively). Although this analysis revealed cell line–specific differences, about 130 PLX4720-responsive genes were commonly up- or downregulated following drug treatment in both cell lines (Fig. 5A). Looking at the 50 most up- or downregulated genes, PLX4720 reduced ERK target gene transcripts such as *FOS* or *IER3* within the first 24 hours (Fig. 5B), again demonstrating long-lasting ERK inhibition. Interestingly, the ERK target gene ERBB receptor feedback inhibitor 1 (*ERRFI1*, Mig-6; ref. 32) was significantly downregulated in both cell lines (Fig. 5B–D). Thus, attenuation of oncogenic B-Raf signaling causes not only the loss of a rapid phosphorylation mediated (19), but also of a delayed negative feedback loop silencing the EGFR via the *de novo* synthesis of an EGFR inhibitor. Furthermore,

Published OnlineFirst November 7, 2014; DOI: 10.1158/0008-5472.CAN-13-3686

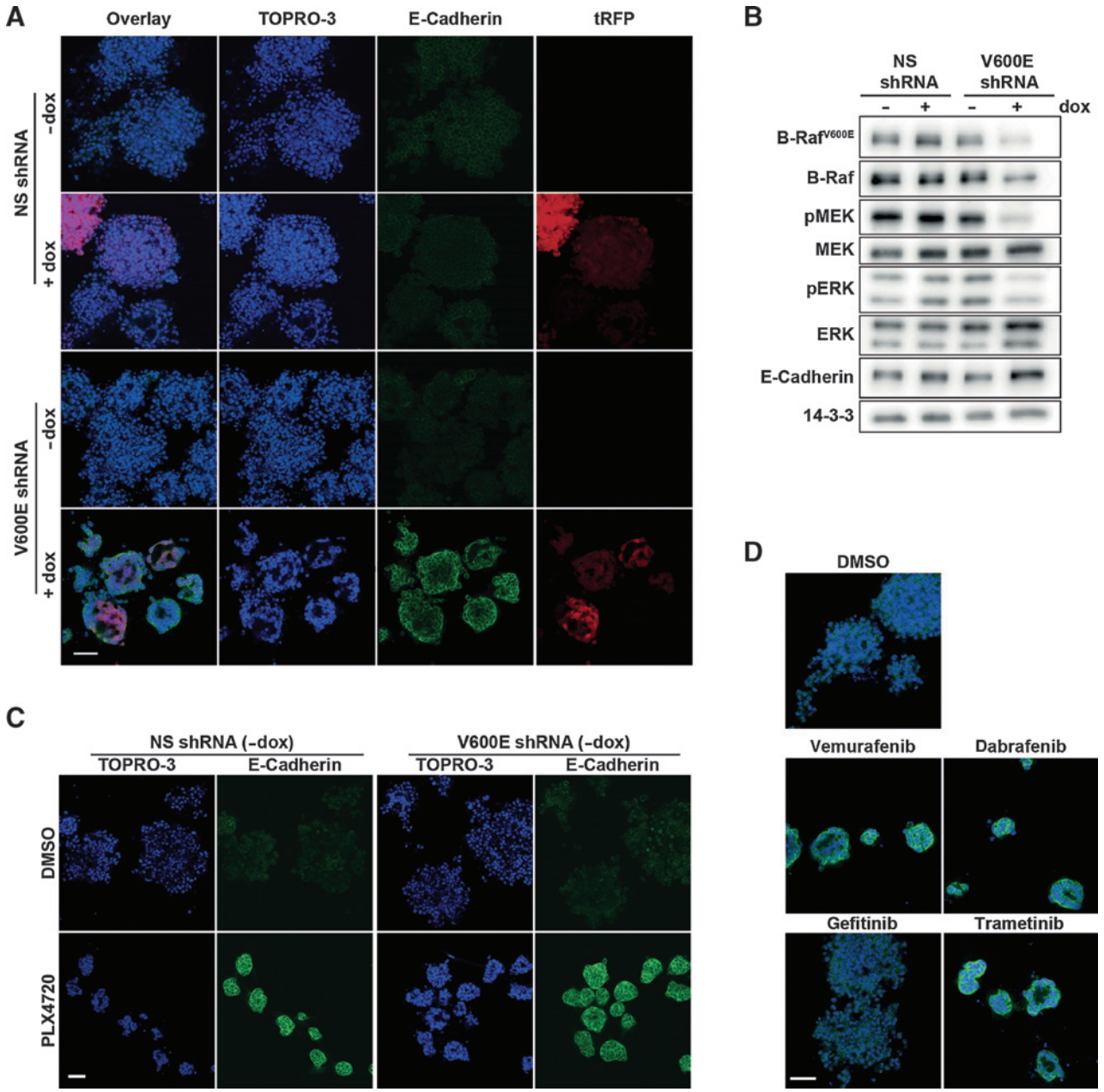

Figure 3.
Inhibition of B-Raf^{V600E} induces spheroid compaction of Colo-205 cells. After 4 days in Matrigel, cultures were subject to B-Raf^{V600E} knockdown or exposed to the indicated inhibitors for 10 days. Cells were stained with E-cadherin and TOPRO-3; scale bar, 50 μm. A, representative confocal images showing compaction and E-cadherin upregulation of doxycyclin (dox)-treated Colo-205/V600E shRNA cells. B, Western blot analysis of 3D cultures of Colo-205 shRNA cells (±dox). C, confocal images showing the scattered clusters of DMSO-treated Colo-205 cells [nonsilencing (NS) and V600E shRNA] and their compaction by PLX4720 treatment (3 μmol/L). D, merged confocal images showing the 3D phenotype of Colo-205/V600E shRNA cells exposed to vemurafenib (3 μmol/L), dabrafenib (1 μmol/L), trametinib (5 nmol/L), gefitinib (1 μmol/L), or DMSO.

we observed a 2.2-fold downregulation of *CDC25C* (Supplementary Table S2). This phosphatase is also phosphorylated in a B-Raf–dependent manner, and thereby responsible for the inefficacy of vemurafenib in many colorectal carcinoma lines (19).

Given these observations in our 3D transcriptomes and the well-established interplay between B-Raf^{V600E} signaling and EGFR activity in conventional tissue culture (19, 20), we next assessed EGFR phosphorylation in spheroid lysates. Interestingly, HT29 cells, which express prominent levels of this receptor tyrosine kinase (RTK; refs. 19, 20), reduce total EGFR levels upon B-Raf^{V600E} knockdown or inhibition (Supplementary Fig. S4C and S4D). However, if this lowered EGFR expression is considered, the phosphorylation of this RTK at its Grb2 recruitment site Y1068 was not significantly increased. This is in full agreement with findings in 2D culture (20), which suggested that vemurafenib allows a better coupling of the EGFR to

Published OnlineFirst November 7, 2014; DOI: 10.1158/0008-5472.CAN-13-3686

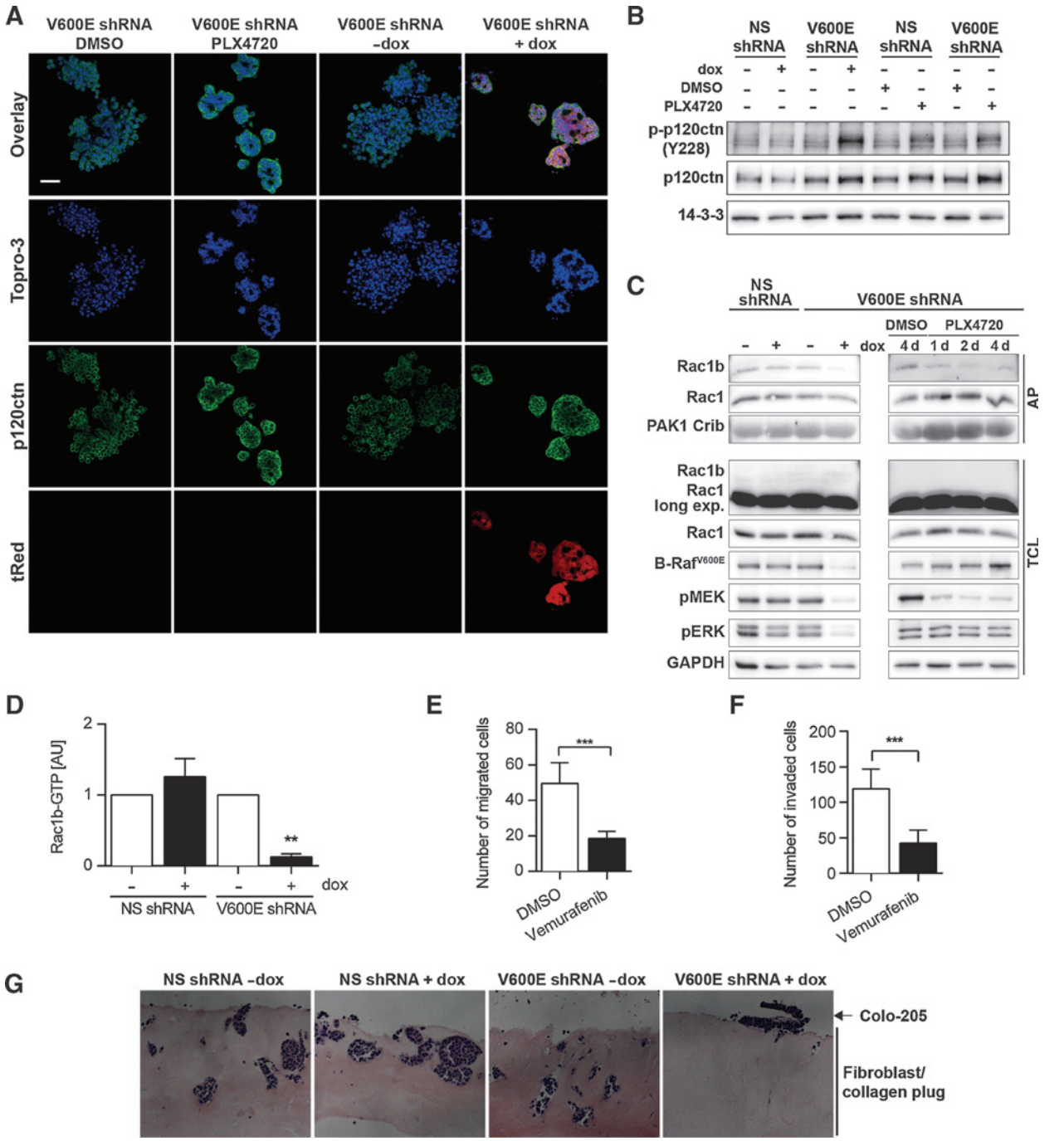

Figure 4.
B-Raf^{V600E} suppresses AJ formation and drives migration and invasion of Colo-205 cells. A, p120ctn was increasingly localized to the membrane upon B-Raf^{V600E} knockdown or inhibition in 3D cultures. Four days after 3D culture set-up, cells were treated ± doxycyclin (dox) or with 3 μmol/L PLX4720 (or DMSO) for 10 days. Cultures were fixed and stained with p120ctn antibodies and TOPRO-3 at day 14; scale bar, 50 μm. B, Western blot analysis of 3D lysates treated as described in A. C, pulldown of GTP-loaded Rac1-GTPases in 2D culture. Knockdown was induced for 4 days or cells were treated with 1 μmol/L PLX4720 or DMSO for up to 4 days. D, statistical analysis of Rac1b-GTP pulldown assays; **, $P < 0.01$. Rac1-GTP levels were not significantly changed (Supplementary Fig. S3D). E and F, Colo-205 cells containing the shRNA control plasmid were pretreated with DMSO or 3 μmol/L vemurafenib and migration/invasion was assessed in Transwell assays after 24 hours; statistical analysis, ***, $P < 0.001$. G, Colo-205 cells were seeded onto a fibroblast/collagen I plug and cultivated for 26 days. Subsequently, the cultures were cut and stained with hematoxylin and eosin. Note that most top layer cells were detached during slicing.

downstream pathways rather than augmenting EGFR activity. In Colo-205 spheroids, however, total EGFR levels were unaffected by B-Raf^{V600E} knockdown or inhibition and, in agreement with other cell lines in 2D culture (19), both treatments augmented Y1068 phosphorylation (Supplementary Fig. S4E). As vemurafenib-mediated reactivation of EGFR signaling

Published OnlineFirst November 7, 2014; DOI: 10.1158/0008-5472.CAN-13-3686

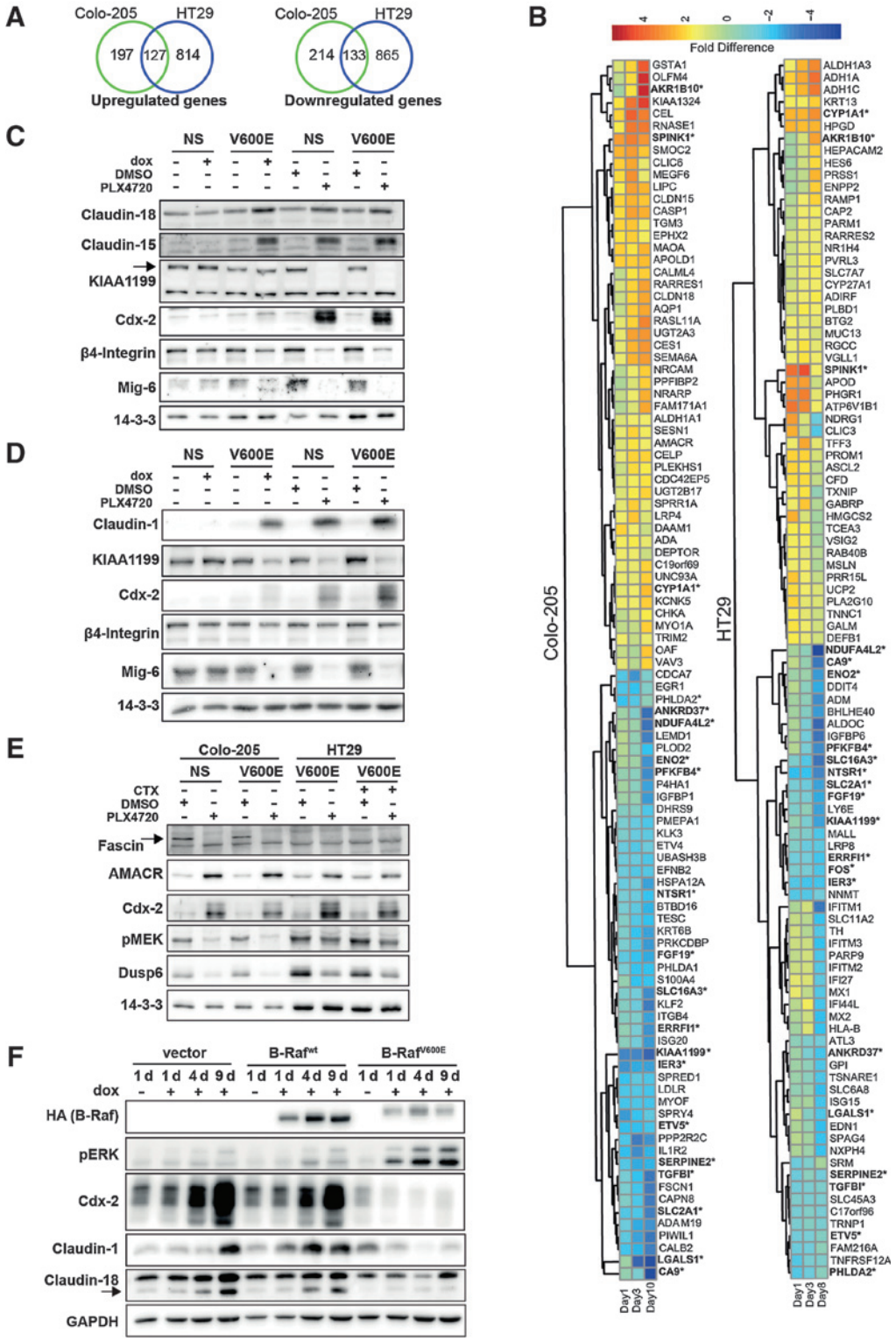

Figure 5.
PLX4720 induces a gene-expression profile associated with epithelial differentiation. 3D cultures were exposed to DMSO/PLX4720 after 4 days in culture. At the indicated time points, cells were subjected to transcriptome analysis. A, Venn diagrams of overlapping differentially regulated genes (moderated *F* test, *q* value < 0.001). B, heatmap of the 50 most up- or downregulated transcripts. Genes differentially regulated in both lines are indicated in bold with asterisks. C, Western blot analysis of Colo-205 cells grown in 3D and treated for 10 days with doxycyclin (dox; ±), DMSO, or 3 μmol/L PLX4720. D, Western blot analysis of HT29 cells grown in 3D and treated for 10 days with dox (±), DMSO, or 3 μmol/L PLX4720 (according to Fig. 2A). E, Western blot analysis of 3D cultures treated as indicated with DMSO, 3 μmol/L PLX4720, and CTX (according to Fig. 2A). F, Caco-2tet lines were grown ±dox for various time points and analyzed by Western blotting.

Published OnlineFirst November 7, 2014; DOI: 10.1158/0008-5472.CAN-13-3686

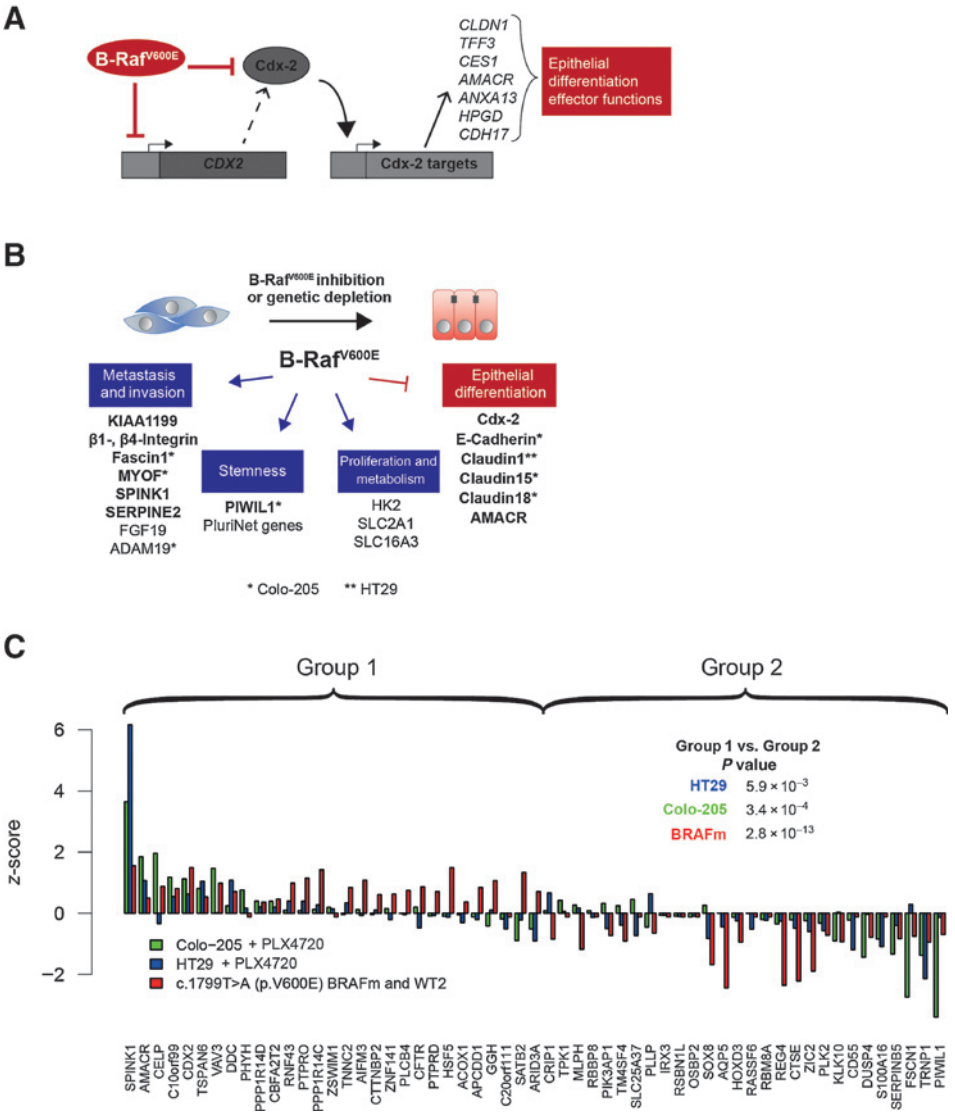

Figure 6.
A, model linking B-Raf^{V600E} signaling to Cdx-2, a master transcription factor for intestinal differentiation. B, model showing how B-Raf^{V600E} impacts on various cancer-related phenomena. For a complete list of differentiation-associated genes, see Supplementary Table S4. Transcripts regulated in Colo-205 and HT29 cells are indicated with one or two asterisks, respectively. Candidates validated by RT-PCR or Western blotting are depicted in bold. C, fold difference of marker genes identified from clinical *BRAF*-mutant colorectal carcinoma specimen. The bar plot depicts the scaled fold change of 64 genes defining the mutant *BRAF* signature (9). Blue and green bars indicate the difference of PLX4720-treated versus untreated HT29 and Colo-205 cells; the red bars indicate the differences of non–*BRAF*- versus *BRAF*-mutant colon cancers. Non–*BRAF*-mutant cells are characterized by high and low expression of genes in groups 1 and 2, respectively. A one-sided *t*- test for differential gene group expression.

augments AKT phosphorylation in 2D culture (19, 20), we next analyzed the phosphorylation status of this kinase at its two key regulatory sites. Similar to 2D tissue culture experiments (19), phosphorylation of S473, an important residue for maximum AKT activation, was increased in HT29 and Colo-205 spheroid lysates. Interestingly, however, phosphorylation of T308, the even more relevant phosphorylation site for AKT activity, was not upregulated, suggesting that B-Raf^{V600E} rather suppresses the mTORC2–AKT than the PDK1–AKT axis (Supplementary Fig. S4C and S4E). These findings represent important details for combination therapies involving antibodies or inhibitors targeting the EGFR.

Importantly, both lines upregulate transcripts explaining the drastic phenotypic changes observed in 3D culture upon loss of B-Raf^{V600E} signaling (Supplementary Table S3). Indeed, many of the top 50 upregulated transcripts (Fig. 5B), for example, *AKR1B10*, *CES*, *HPGD*, *RARRES1*, *TFF3*, or *TXNIP*, are linked to epithelial differentiation and effector functions (Supplementary Table S4). Moreover, the master transcription factor of intestinal development and epithelial differentiation, Cdx-2, was significantly upregulated in Colo-205 and HT29 cells by PLX4720 treatment at the transcript (Supplementary Table S2) and protein level (Fig. 5C–E). As shown in Fig. 6A, this is also reflected by the upregulation of various previously identified Cdx-2 targets (33). For example, AMACR, a potential Cdx-2 target and marker for differentiated colorectal carcinomas, was upregulated in HT29 and Colo-205 cells (Fig. 5B and E) and also in three additional *BRAF*^{V600E}-mutant colorectal carcinoma lines (Colo-201, LS411, and HDC135), which we used for additional follow-up (Supplementary Fig. S4F). Furthermore, the TJ components claudin-15 (*CLDN15*) and claudin-18 (*CLDN18*) were upregulated in Colo-205 cells following B-Raf^{V600E} inhibition or knockdown. Interestingly, these claudins were not prominently upregulated in HT29 cells, in which we observed a significant induction of claudin-1 (*CLDN1*; Fig. 5C and D and Supplementary Fig. S5A–S5C). The reciprocal relationship between B-Raf^{V600E} and Cdx-2, claudin-1 and -18 was further confirmed in Caco-2tet cells, which spontaneously differentiate with increasing confluency. Here, these proteins were upregulated in cultures transfected with the empty and

Published OnlineFirst November 7, 2014; DOI: 10.1158/0008-5472.CAN-13-3686

B-Raf^{wt} expression vectors, whereas B-Raf^{V600E} expression counteracted their upregulation (Fig. 5F).

Conversely, PLX4720 suppressed transcripts promoting migration and invasion. For example, β4-integrin (*ITGB*4), which was induced by B-Raf^{V600E} in Caco-2tet cells and contributes to colorectal tumor progression (34), was reduced in Colo-205 and to a lesser extent in HT29 cells (Fig. 5C and D and Supplementary Table S2). Furthermore, Fascin1 (*FSCN*1), a gene increasingly implicated in metastasis (35), was downregulated at the transcript level in Colo-205 and at the protein level in Colo-201, Colo-205, and LS411 cells (Fig. 5B and E and Supplementary Fig. S4F). In full agreement with a previous study linking Fascin1 to loss of differentiation (35), HT29 cells lacked Fascin1 expression (Fig. 5E). Likewise, myoferlin (*MYOF*), a gene linked to breast cancer progression (36) and metastasis of pancreatic carcinoma (37), was downregulated in Colo-205 cells (Fig. 5B and Supplementary Fig. S6A). B-Raf inhibition also altered the expression levels of transcripts controlling proteolytic processes. For example, *ADAM*19 and *KLK*3 were reduced in PLX4720-treated Colo-205 cells. Likewise, *SERPINE*2, which represents a promoter of tumor progression and metastasis in many tumor entities, was downregulated in both cell types. Conversely, the protease inhibitor *SPINK*1, an inhibitor of invasive processes and marker for a favorable prognosis in patients with colorectal carcinoma (38), was upregulated in both cell lines (Fig. 5B and Supplementary Fig. S6A). Importantly, our analyses also identified PLX4720-suppressed transcripts such as *FGF19* and *KIAA1199* (Fig. 5B–D and Supplementary Figs. S4F and S6A). Both are discussed as markers for poor prognosis in several entities (39, 40).

Furthermore, we identified transcripts in Colo-205 cells associated with stemness: *PIWIL*1, a critical epigenetic regulator implicated in self-renewal of normal and cancer stem cells (41), was strongly downregulated by PLX4720 (Fig. 5B and Supplementary Fig. S6A). Interestingly, transcripts of two genes controversially discussed as stemness markers, *SMOC*2 and *OLFM*4 (42), were upregulated by PLX4720 (Fig. 5B and Supplementary Fig. S6A). However, the well-established markers of intestinal crypts such as *LGR*5 and *BMI* (42) were not affected by PLX4720 (Supplementary Table S2) arguing against the induction of stemness. In fact, both cell lines loose stemness-associated transcripts following B-Raf inhibition (Supplementary Fig. S6B). The diverse cancer-related processes affected by PLX4720 treatment are summarized in Fig. 6B.

Next, we compared the PLX4720 response of both cell lines with clinical data, in which a 64–gene-expression signature for *BRAF*-mutant colorectal carcinomas was established (9). We mapped 57 of the 64 genes onto our transcriptome data, illustrating the similarities of our 3D cell culture systems with the *in vivo* transcriptomes of clinical colorectal carcinoma samples. By plotting the mean fold change after PLX4720 treatment individually for both classifier gene groups, a significant differential gene regulation over time was observed (Fig. 6C). Importantly, this classifier comprises several of the most-regulated transcripts of PLX4720-treated spheroids such as *SPINK*1, *AMACR*, *CDX*2, *FSCN*1, and *PIWIL*1. This demonstrates how the *in vitro* transcriptome of both lines switches from a transcriptome reflecting *BRAF*-mutant colorectal carcinomas toward one based on tumors lacking this mutation. Thus, many transcriptional alterations typically observed in clinical *BRAF*-mutant colorectal carcinoma samples might be reversible by pharmacologic intervention.

B-Raf^{V600E} suppresses hallmarks of intestinal differentiation *in vivo*

To analyze the role of oncogenic B-Raf signaling *in vivo*, xenograft experiments with HT29 cells containing nonsilencing or V600E shRNA constructs were performed. Doxycycline administration (starting at d7) stalled the growth of xenografts containing the V600E-specific shRNA construct, whereas tumors in the doxycycline-treated nonsilencing group or in both untreated groups grew exponentially (Fig. 7A and Supplementary Fig. S6C). Strikingly, B-Raf^{V600E} knockdown induced the formation of glandular structures (Fig. 7B), which was further confirmed by periodic acid-Schiff (PAS) and Cdx-2 staining (2, 43, 44). Importantly, glandular differentiation was not observed in the three control groups maintaining B-Raf^{V600E} expression. Doxycycline administration to HT29/V600E shRNA carrying mice reduced the number of cells expressing the proliferation marker Ki-67. In agreement with earlier studies (16, 17), tumor regression was also observed in mice treated with vemurafenib or trametinib (Fig. 7C). Furthermore, differentiated areas were observed in most vemurafenib-treated xenografts, albeit to various degrees (Fig. 7D). In agreement with the high efficacy of MEK inhibitors in colorectal carcinoma lines (16), glandular differentiation was more advanced and visible in all trametinib-treated xenografts. In both drug-treated xenograft groups, glandular differentiation was confirmed by PAS and Cdx-2 staining. Importantly, glandular differentiation was not observed in any of the DMSO-treated xenografts. Thus, the differentiation-suppressing effect of B-Raf^{V600E}/MEK/ERK signaling observed *in vitro* can be reproduced in xenografts *in vivo*.

Discussion

BRAF^{V600E} confers a poor prognosis to patients with MSS colorectal carcinomas (8–10) and increases peritoneal metastasis (11, 12). However, the molecular and cellular mechanisms underlying these correlations remain ill-defined as most studies addressed oncogenic B-Raf in terms of its impact on colorectal carcinoma initiation by focusing on proliferation and survival (4, 19). Furthermore, studies relied on the phenotypic comparison of cell lines or tumors with either wild-type or mutant *BRAF* status, which, although insightful, only allows drawing conclusions of correlative nature. Here, we generated three conditional human colorectal carcinoma cell line models, which allow us to directly analyze the acute influence of B-Raf^{V600E} within an isogenic setting. We demonstrate that B-Raf^{V600E} enhances migration and invasion, impairs cellular junctions and controls epithelial differentiation markers of prognostic relevance.

For example, B-Raf^{V600E} suppresses the function of TJ, a hallmark of intestinal epithelia. We demonstrate that reduction of chronic B-Raf/MEK signaling induces large lumina upon CTX exposure, suggesting an improved sealing of cell–cell contacts. However, the expression and/or localization of critical TJ components or regulators, such as occludin, ZO-1 or scribble were not altered (Supplementary Fig. S6D and S6E and data not shown). This suggests that, in the presence of B-Raf^{V600E}, HT29 cells are able to form rudimentary but "leaky" TJs in which not all critical components are properly localized or expressed. Indeed, we demonstrate for the first time that B-Raf^{V600E} suppresses the expression of three distinct claudins. In HT29 cells, knockdown or inhibition of B-Raf^{V600E} upregulated the barrier forming and sealing claudin-1. Conversely, B-Raf^{V600E} strongly reduces

Published OnlineFirst November 7, 2014; DOI: 10.1158/0008-5472.CAN-13-3686

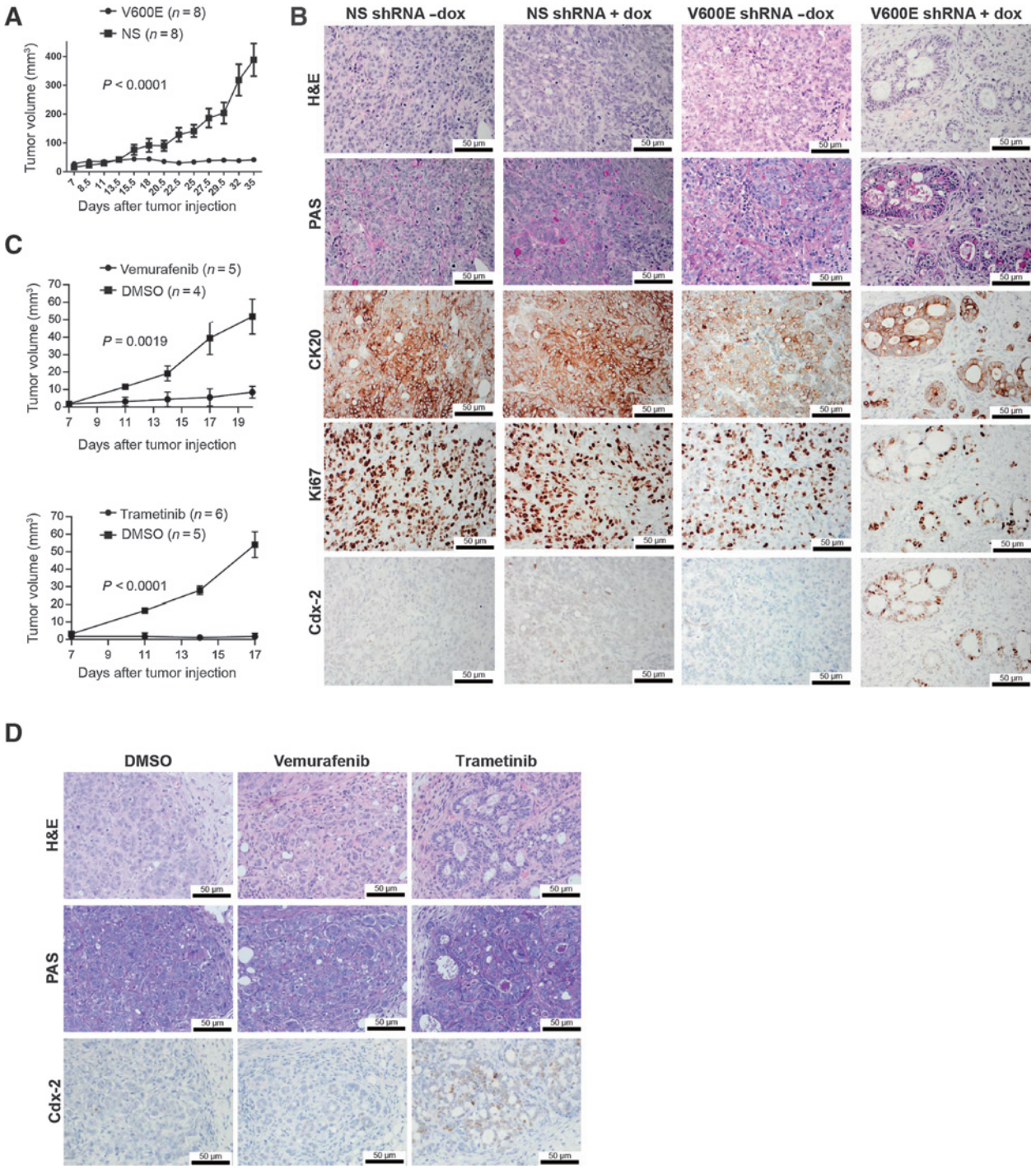

Figure 7.
B-Raf^{V600E} loss stalls tumor growth and induces glandular differentiation of HT29 cells *in vivo*. A, growth of subcutaneous HT29 xenografts containing the nonsilencing (NS) or V600E shRNA was monitored over time. B, histologic analysis of xenografts. H&E, hematoxylin and eosin stains; CK20, human cytokeratin 20; Ki67, proliferation marker; scale bar, 50 μm. CK20 distinguishes the xenograft from murine stroma. C, xenograft growth of vemurafenib- (70 mg/kg, twice daily) and trametinib (1 mg/kg, daily)-treated mice. Seven days after tumor injection, inhibitors were applied by oral gavage for 13 and 10 days, respectively. D, xenograft histology of inhibitor-treated mice (treated as described in C). Note the increased mucin production and ductal differentiation in vemurafenib- and more prominently in trametinib-treated mice.

claudin-1 in Caco-2tet cells, which provides an additional mechanism as to how this oncoprotein interferes with the development and maintenance of epithelial cysts (23, 45).

Unlike HT29 cells, Colo-205 spheroids with B-Raf^{V600E} knockdown or inhibition lack CTX-induced lumina, despite their prominent compaction phenotype (data not shown).

Published OnlineFirst November 7, 2014; DOI: 10.1158/0008-5472.CAN-13-3686

Interestingly, Colo-205 cells with B-Raf^{V600E} knockdown or inhibition upregulated the pore-forming claudin-15 and -18, which contribute to cell–cell adhesion, and thereby fulfill a critical function in gastrointestinal development (46). Thus, these claudins, together with the sequestration of p120ctn into the reformed AJs (Fig. 4A and B), an event known to counteract the proinvasive character of free p120ctn (31), might contribute to the compaction of Colo-205 spheroids.

But how does B-Raf^{V600E} suppress claudins? To our knowledge, nothing is known about the mechanism regulating claudin-15 and -18 expression. Thus, our analyses connect these lesser-characterized claudins to B-Raf^{V600E} signaling. In contrast, there is a controversy about the mechanisms underlying claudin-1 expression. For example, the NF-κB, Wnt-, and MEK/ERK pathways as well as Snail1, Cdx-1/2, and Gata-4 are implicated in *CLDN*1 transcription (46, 47). Thus, our finding that claudin-1 is strongly suppressed by endogenous B-Raf^{V600E} links its expression to a clinically relevant oncogenic driver.

A major finding of our study is that the presence of B-Raf^{V600E} suppresses *CDX2* expression at the transcript and protein levels in our three isogenic colorectal carcinoma cell line models. B-Raf or MEK inhibition also induced Cdx-2 expression in MSS (HT29 and Colo-205) and MSI (LS411 and HDC135) cells. Importantly, this phenomenon was also observed in HT29 xenografts, which presented with Cdx-2–positive glandular epithelial structures upon B-Raf^{V600E} knockdown or treatment with trametinib and, albeit to a lesser degree, with vemurafenib. Cdx-2 represents a master transcription factor regulating the differentiation, cell–cell adhesion, and polarity of intestinal epithelia (48), and indeed we observe several Cdx-2 targets being upregulated by B-Raf/MEK inhibition (Figs. 5B and 6A). The mechanisms controlling Cdx-2 expression are controversially discussed and implicate the Wnt, Notch, JNK, and ERK pathways as well as epithelial–mesenchymal transition regulators, epigenetic mechanisms, and the tumor microenvironment (7, 43, 48, 49). Interestingly, knockdown of Cdx-2 in Caco-2 cells disrupts cyst development (50), whereas its ectopic expression in Colo-205 cells improved E-cadherin function and cell–cell adhesion in 2D culture (51). Thus, both studies report phenocopies of experiments involving the ectopic expression or knockdown of B-Raf^{V600E} in Caco-2 cysts (23, 45) and Colo-205 cells (Fig. 3), respectively. These striking parallels imply that many aspects of the transformed phenotype evoked by B-Raf^{V600E} are mediated by Cdx-2 loss. Our identification of endogenous B-Raf^{V600E} as a Cdx-2 suppressor has clinical implications, because its loss is observed at the invasive front and is implicated in metastasis (43). Indeed, loss of Cdx-2 forecasts a poor prognosis and is frequently observed in right-sided colorectal carcinomas, which display a particularly high *BRAF* mutation rate (2, 44, 52). Furthermore, loss of Cdx-2 expression in MSI and MSS colorectal carcinoma tissue specimens is strongly correlated with *BRAF*^{V600E} and higher tumor grade (7, 53). Likewise, loss of expression of the Cdx-2 target gene *CLDN*1, which we identified as a B-Raf^{V600E} repressed gene, strongly predicts disease recurrence and poor patient survival (54). Thus, our isogenic model systems now provide a mechanism for the correlation between *BRAF* mutation status, Cdx-2, and claudin-1 expression by showing a dynamic and inverse relationship between B-Raf^{V600E} and the expression of Cdx-2 and its targets such as *CLDN1* and *AMACR* (Figs. 5A and 6A). As Cdx-2 positively regulates a plethora of differentiation markers (Supplementary Table S4), our study suggests a mechanism for the aforementioned poor differentiation status (1, 2, 11). The differentiation-suppressing effect of oncogenic B-Raf is of particular interest in relation to recent studies reporting a novel classification system for colorectal carcinomas based on gene-expression profiling (1, 2). These studies show that *BRAF*-mutant colorectal carcinomas tend to be less differentiated and often display a stem-like signature.

To our knowledge, we are the first to describe the transcriptional alterations induced by a B-Raf inhibitor in 3D cultures of two colorectal carcinoma cell lines with an endogenous *BRAF*^{V600E} mutation. This identified transcripts associated with cellular adhesion, invasion, and metastasis, which might represent potential prognostic colorectal carcinoma markers. Several of these alterations at the transcript level were reflected at the protein level, not only in the profiled HT29 and Colo-205 cells but also in other colorectal carcinoma lines (Supplementary Fig. S4F). Some of these transcripts are known from other tumor entities, but have neither been implicated in colorectal carcinoma nor connected to B-Raf signaling. For example, although Fascin1 has been implicated as a Wnt target gene in colorectal carcinoma (35), our data show that B-Raf inhibition is sufficient to block the expression of this metastasis gene.

Furthermore, we identified B-Raf^{V600E} targets of ill-defined or unknown function. For example, KIAA1199 was significantly downregulated by B-Raf or MEK inhibition. KIAA1199 emerges as a marker of poor prognosis in several tumor entities, including colorectal carcinoma, but has never been linked to *BRAF* mutations before (39, 40, 55). Its activity as a promoter of cell migration in noncolorectal carcinoma cell lines (55) fits well to the strong reduction of invasive behavior of Colo-205 cells with inhibition or knockdown of B-Raf^{V600E}.

Thus, the identification of the mechanisms and cooperating signaling pathways by which oncogenic B-Raf suppresses differentiation and cell–cell adhesion represents a future task. Collectively, we show that B-Raf^{V600E} inhibition reduces the expression of transcripts associated with negative diagnostic value and increases those forecasting a more favorable outcome. Moreover, the datasets derived from our dynamic isogenic experimental systems complement gene-expression studies based on the comparison of clinical and therefore heterogeneous tumor samples (1, 2, 9).

Our discovery that B-Raf^{V600E} inhibition improves cell–cell adhesion by restoring AJs and TJs, impairs migration and invasion, and increases hallmarks of epithelial differentiation identifies a novel facet of inhibitors targeting the B-Raf/MEK/ERK pathway (Fig. 6B). Importantly, trametinib, which is part of combination therapies trialed in colorectal carcinoma, yields the same effects as B-Raf inhibitors in our 3D cultures and xenograft experiments. This implicates MEK as a key mediator of the differentiation suppression exerted by B-Raf^{V600E}. Although clearly beyond the scope of the present study, it would be interesting to assess the sensitivity of our isogenic cell line models toward conventional chemotherapy compounds, because differentiation status is often correlated with drug responses. Taken together, our study highlights the possibility for a novel therapeutic rationale for using B-Raf/MEK/ERK pathway inhibitors in colorectal carcinoma and potentially other carcinoma entities. Thus, these drugs could potentially limit metastasis, most likely, in combination with conventional chemotherapy or other targeted therapy compounds such as EGFR or dual PI3K/mTOR inhibitors (4, 17–20). Such combinations, which target various hallmarks of cancer, are currently in clinical trials for colorectal carcinoma. It will be

interesting to see whether a differentiation-promoting effect can be observed in these clinical settings.

Disclosure of Potential Conflicts of Interest

No potential conflicts of interest were disclosed.

Authors' Contributions

Conception and design: R. Herr, M.A. Olayioye, H. Busch, M. Boerries, T. Brummer

Development of methodology: R. Herr, H. Andrlová, Y. Möller, N. Bittermann, S. Lassmann, T. Brummer

Acquisition of data (provided animals, acquired and managed patients, provided facilities, etc.): R. Herr, M. Köhler, H. Andrlová, F. Weinberg, Y. Möller, S. Halbach, M. Klose, N. Bittermann, S. Kowar, R. Zeiser, S. Lassmann, T. Brummer

Analysis and interpretation of data (e.g., statistical analysis, biostatistics, computational analysis): R. Herr, M. Köhler, H. Andrlová, F. Weinberg, Y. Möller, S. Halbach, N. Bittermann, R. Zeiser, M.A. Olayioye, S. Lassmann, H. Busch, M. Boerries, T. Brummer

Writing, review, and/or revision of the manuscript: R. Herr, M. Köhler, F. Weinberg, S. Halbach, R. Zeiser, M.A. Olayioye, S. Lassmann, H. Busch, M. Boerries, T. Brummer

Administrative, technical, or material support (i.e., reporting or organizing data, constructing databases): J. Mastroianni, S. Kowar, H. Busch, M. Boerries, T. Brummer

Study supervision: T. Brummer

Other (evaluation and interpretation of histology): L. Lutz

Acknowledgments

The authors thank Martin Werner for supporting histologic and immunohistochemical xenograft analyses, and Paul Timpson for discussion.

Grant Support

This work was funded by the DFG *via* the Collaborative Research Centre 850 (projects B4, C5, C6, Z1, and Z2), the *Emmy-Noether*-Program (T. Brummer) and SPP1395/InKomBio (M. Boerries, H. Busch, and M. Köhler). The Excellence Initiative of the German Federal and State Governments supports T. Brummer (EXC 294 BIOSS), and M. Köhler and S. Halbach (GSC-4; SGBM). This study was also supported by the BMBF through e:Bio 0316184D.

The costs of publication of this article were defrayed in part by the payment of page charges. This article must therefore be hereby marked *advertisement* in accordance with 18 U.S.C. Section 1734 solely to indicate this fact.

Received December 29, 2013; revised October 2, 2014; accepted October 14, 2014; published OnlineFirst November 7, 2014.

References

1. Sadanandam A, Lyssiotis CA, Homicsko K, Collisson EA, Gibb WJ, Wullschleger S, et al. A colorectal cancer classification system that associates cellular phenotype and responses to therapy. Nat Med 2013;19:619–25.
2. De Sousa EMF, Wang X, Jansen M, Fessler E, Trinh A, de Rooij LP, et al. Poor-prognosis colon cancer is defined by a molecularly distinct subtype and develops from serrated precursor lesions. Nat Med 2013;19:614–8.
3. Clancy C, Burke JP, Kalady MF, Coffey JC. BRAF mutation is associated with distinct clinicopathological characteristics in colorectal cancer: a systematic review and meta-analysis. Colorectal Dis 2013;15:e711–8.
4. Rad R, Cadinanos J, Rad L, Varela I, Strong A, Kriegl L, et al. A genetic progression model of braf-induced intestinal tumorigenesis reveals targets for therapeutic intervention. Cancer Cell 2013;24:15–29.
5. Sinicrope FA, Shi Q, Thibodeau SN, Goldberg RM, Sargent DJ, Alberts SR. Molecular subtyping of colon cancers and distinct prognostic groups [NCCTG N0147 (Alliance)]. J Clin Oncol 32:5s, 2014 (suppl; abstr 3512).
6. Roth AD, Delorenzi M, Tejpar S, Yan P, Klingbiel D, Fiocca R, et al. Integrated analysis of molecular and clinical prognostic factors in stage II/III colon cancer. J Natl Cancer Inst 2012;104:1635–46.
7. Landau MS, Kuan SF, Chiosea S, Pai RK. BRAF-mutated microsatellite stable colorectal carcinoma: an aggressive adenocarcinoma with reduced CDX2 and increased cytokeratin 7 immunohistochemical expression. Hum Pathol 2014;45:1704–12.
8. Pai RK, Jayachandran P, Koong AC, Chang DT, Kwok S, Ma L, et al. BRAF-mutated, microsatellite-stable adenocarcinoma of the proximal colon: an aggressive adenocarcinoma with poor survival, mucinous differentiation, and adverse morphologic features. Am J Surg Pathol 2012;36:744–52.
9. Popovici V, Budinska E, Tejpar S, Weinrich S, Estrella H, Hodgson G, et al. Identification of a poor-prognosis BRAF-mutant-like population of patients with colon cancer. J Clin Oncol 2012;30:1288–95.
10. Tie J, Gibbs P, Lipton L, Christie M, Jorissen RN, Burgess AW, et al. Optimizing targeted therapeutic development: analysis of a colorectal cancer patient population with the BRAF(V600E) mutation. Int J Cancer 2011;128:2075–84.
11. Yaeger R, Cercek A, Chou JF, Sylvester BE, Kemeny NE, Hechtman JF, et al. BRAF mutation predicts for poor outcomes after metastasectomy in patients with metastatic colorectal cancer. Cancer 2014;120:2316–24.
12. Tran B, Kopetz S, Tie J, Gibbs P, Jiang ZQ, Lieu CH, et al. Impact of BRAF mutation and microsatellite instability on the pattern of metastatic spread and prognosis in metastatic colorectal cancer. Cancer 2011;117:4623–32.
13. Bollag G, Hirth P, Tsai J, Zhang J, Ibrahim PN, Cho H, et al. Clinical efficacy of a RAF inhibitor needs broad target blockade in BRAF-mutant melanoma. Nature 2010;467:596–9.
14. Falchook GS, Long GV, Kurzrock R, Kim KB, Arkenau TH, Brown MP, et al. Dabrafenib in patients with melanoma, untreated brain metastases, and other solid tumours: a phase 1 dose-escalation trial. Lancet 2012;379:1893–901.
15. Morris V, Kopetz S. BRAF inhibitors in clinical oncology. F1000prime Rep 2013;5:11.
16. Yamaguchi T, Kakefuda R, Tajima N, Sowa Y, Sakai T. Antitumor activities of JTP-74057 (GSK1120212), a novel MEK1/2 inhibitor, on colorectal cancer cell lines in vitro and in vivo. Int J Oncol 2011;39:23–31.
17. Yang H, Higgins B, Kolinsky K, Packman K, Bradley WD, Lee RJ, et al. Antitumor activity of BRAF inhibitor vemurafenib in preclinical models of BRAF-mutant colorectal cancer. Cancer Res 2012;72:779–89.
18. Coffee EM, Faber AC, Roper J, Sinnamon MJ, Goel G, Keung L, et al. Concomitant BRAF and PI3K/mTOR blockade is required for effective treatment of BRAF(V600E) colorectal cancer. Clin Cancer Res 2013;19:2688–98.
19. Prahallad A, Sun C, Huang S, Di Nicolantonio F, Salazar R, Zecchin D, et al. Unresponsiveness of colon cancer to BRAF(V600E) inhibition through feedback activation of EGFR. Nature 2012;483:100–3.
20. Corcoran RB, Ebi H, Turke AB, Coffee EM, Nishino M, Cogdill AP, et al. EGFR-mediated re-activation of MAPK signaling contributes to insensitivity of BRAF mutant colorectal cancers to RAF inhibition with vemurafenib. Cancer Discov 2012;2:227–35.
21. Misale S, Arena S, Lamba S, Siravegna G, Lallo A, Hobor S, et al. Blockade of EGFR and MEK intercepts heterogeneous mechanisms of acquired resistance to anti-EGFR therapies in colorectal cancer. Sci Translational Med 2014;6:224ra26.
22. Connolly K, Brungs D, Szeto E, Epstein RJ. Anticancer activity of combination targeted therapy using cetuximab plus vemurafenib for refractory BRAF (V600E)-mutant metastatic colorectal carcinoma. Curr Oncol 2014;21:e151–4.
23. Röring M, Herr R, Fiala GJ, Heilmann K, Braun S, Eisenhardt AE, et al. Distinct requirement for an intact dimer interface in wild-type, V600E and kinase-dead B-Raf signalling. EMBO J 2012;31:2629–47.
24. Herr R, Wohrle FU, Danke C, Berens C, Brummer T. A novel MCF-10A line allowing conditional oncogene expression in 3D culture. Cell Commun Signal 2011;9:17.
25. Timpson P, McGhee EJ, Erami Z, Nobis M, Quinn JA, Edward M, et al. Organotypic collagen I assay: a malleable platform to assess cell behaviour in a 3-dimensional context. J Vis Exp 2011;56:e3089.
26. Hoffmann C, Pop M, Leemhuis J, Schirmer J, Aktories K, Schmidt G. The Yersinia pseudotuberculosis cytotoxic necrotizing factor (CNFY) selectively activates RhoA. J Biol Chem 2004;279:16026–32.

Published OnlineFirst November 7, 2014; DOI: 10.1158/0008-5472.CAN-13-3686

27. Gout S, Marie C, Laine M, Tavernier G, Block MR, Jacquier-Sarlin M. Early enterocytic differentiation of HT-29 cells: biochemical changes and strength increases of adherens junctions. Exp Cell Res 2004;299:498–510.
28. Esufali S, Charames GS, Pethe VV, Buongiorno P, Bapat B. Activation of tumor-specific splice variant Rac1b by dishevelled promotes canonical Wnt signaling and decreased adhesion of colorectal cancer cells. Cancer Res 2007;67:2469–79.
29. Jaffe AB, Kaji N, Durgan J, Hall A. Cdc42 controls spindle orientation to position the apical surface during epithelial morphogenesis. J Cell Biol 2008;183:625–33.
30. Pratilas CA, Taylor BS, Ye Q, Viale A, Sander C, Solit DB, et al. (V600E)BRAF is associated with disabled feedback inhibition of RAF-MEK signaling and elevated transcriptional output of the pathway. Proc Natl Acad Sci U S A 2009;106:4519–24.
31. Pieters T, van Roy F, van Hengel J. Functions of p120ctn isoforms in cell-cell adhesion and intracellular signaling. Front Biosci 2012;17:1669–94.
32. Ferby I, Reschke M, Kudlacek O, Knyazev P, Pante G, Amann K, et al. Mig6 is a negative regulator of EGF receptor-mediated skin morphogenesis and tumor formation. Nat Med 2006;12:568–73.
33. Hinoi T, Gesina G, Akyol A, Kuick R, Hanash S, Giordano TJ, et al. CDX2-regulated expression of iron transport protein hephaestin in intestinal and colonic epithelium. Gastroenterology 2005;128:946–61.
34. Ni H, Dydensborg AB, Herring FE, Basora N, Gagne D, Vachon PH, et al. Upregulation of a functional form of the beta4 integrin subunit in colorectal cancers correlates with c-Myc expression. Oncogene 2005;24:6820–9.
35. Vignjevic D, Schoumacher M, Gavert N, Janssen KP, Jih G, Lae M, et al. Fascin, a novel target of beta-catenin-TCF signaling, is expressed at the invasive front of human colon cancer. Cancer Res 2007;67:6844–53.
36. Turtoi A, Blomme A, Bellahcene A, Gilles C, Hennequiere V, Peixoto P, et al. Myoferlin is a key regulator of EGFR activity in breast cancer. Cancer Res 2013;73:5438–48.
37. Wang WS, Liu XH, Liu LX, Lou WH, Jin DY, Yang PY, et al. iTRAQ-based quantitative proteomics reveals myoferlin as a novel prognostic predictor in pancreatic adenocarcinoma. J Proteomics 2013;91C:453–65.
38. Koskensalo S, Hagstrom J, Louhimo J, Stenman UH, Haglund C. Tumour-associated trypsin inhibitor TATI is a prognostic marker in colorectal cancer. Oncology 2012;82:234–41.
39. Sabates-Bellver J, Van der Flier LG, de Palo M, Cattaneo E, Maake C, Rehrauer H, et al. Transcriptome profile of human colorectal adenomas. Mol Cancer Res 2007;5:1263–75.
40. Birkenkamp-Demtroder K, Maghnouj A, Mansilla F, Thorsen K, Andersen CL, Oster B, et al. Repression of KIAA1199 attenuates Wnt-signalling and decreases the proliferation of colon cancer cells. Br J Cancer 2011;105:552–61.
41. Siddiqi S, Matushansky I. Piwis and piwi-interacting RNAs in the epigenetics of cancer. J Cell Biochem 2012;113:373–80.
42. Ziskin JL, Dunlap D, Yaylaoglu M, Fodor IK, Forrest WF, Patel R, et al. *In situ* validation of an intestinal stem cell signature in colorectal cancer. Gut 2013;62:1012–23.
43. Brabletz T, Spaderna S, Kolb J, Hlubek F, Faller G, Bruns CJ, et al. Down-regulation of the homeodomain factor Cdx2 in colorectal cancer by collagen type I: an active role for the tumor environment in malignant tumor progression. Cancer Res 2004;64:6973–7.
44. Baba Y, Nosho K, Shima K, Freed E, Irahara N, Philips J, et al. Relationship of CDX2 loss with molecular features and prognosis in colorectal cancer. Clin Cancer Res 2009;15:4665–73.
45. Magudia K, Lahoz A, Hall A. K-Ras and B-Raf oncogenes inhibit colon epithelial polarity establishment through up-regulation of c-myc. J Cell Biol 2012;198:185–94.
46. Gunzel D, Yu AS. Claudins and the modulation of tight junction permeability. Physiol Rev 2013;93:525–69.
47. Bhat AA, Sharma A, Pope J, Krishnan M, Washington MK, Singh AB, et al. Caudal homeobox protein Cdx-2 cooperates with Wnt pathway to regulate claudin-1 expression in colon cancer cells. PloS ONE 2012;7:e37174.
48. Krueger F, Madeja Z, Hemberger M, McMahon M, Cook SJ, Gaunt SJ. Down-regulation of Cdx2 in colorectal carcinoma cells by the Raf-MEK-ERK 1/2 pathway. Cell Signal 2009;21:1846–56.
49. Gross I, Duluc I, Benameur T, Calon A, Martin E, Brabletz T, et al. The intestine-specific homeobox gene Cdx2 decreases mobility and antagonizes dissemination of colon cancer cells. Oncogene 2008;27:107–15.
50. Gao N, Kaestner KH. Cdx2 regulates endo-lysosomal function and epithelial cell polarity. Genes Dev 2010;24:1295–305.
51. Funakoshi S, Kong J, Crissey MA, Dang L, Dang D, Lynch JP. Intestine-specific transcription factor Cdx2 induces E-cadherin function by enhancing the trafficking of E-cadherin to the cell membrane. Am J Physiol Gastrointest Liver Physiol 2010;299:G1054–67.
52. Zlobec I, Bihl MP, Schwarb H, Terracciano L, Lugli A. Clinicopathological and protein characterization of BRAF- and K-RAS-mutated colorectal cancer and implications for prognosis. Int J Cancer 2010;127:367–80.
53. Dawson H, Galvan JA, Helbling M, Muller DE, Karamitopoulou E, Koelzer VH, et al. Possible role of Cdx2 in the serrated pathway of colorectal cancer characterized by BRAF mutation, high-level CpG Island methylator phenotype and mismatch repair-deficiency. Int J Cancer 2014;134:2342–51.
54. Resnick MB, Konkin T, Routhier J, Sabo E, Pricolo VE. Claudin-1 is a strong prognostic indicator in stage II colonic cancer: a tissue microarray study. Mod Pathol 2005;18:511–8.
55. Evensen NA, Kuscu C, Nguyen HL, Zarrabi K, Dufour A, Kadam P, et al. Unraveling the role of KIAA1199, a novel endoplasmic reticulum protein, in cancer cell migration. J Natl Cancer Inst 2013;105:1402–16.

Cancer Research
The Journal of Cancer Research (1916–1930) | The American Journal of Cancer (1931–1940)

AACR American Association for Cancer Research

B-Raf Inhibitors Induce Epithelial Differentiation in *BRAF*-Mutant Colorectal Cancer Cells

Ricarda Herr, Martin Köhler, Hana Andrlová, et al.

Cancer Res Published OnlineFirst November 7, 2014.